Published in final edited form as:
Braz J Med Biol Res. 2009 January ; 42(1): 94–104.

Synaptic vesicle pool size, release probability and synaptic depression are sensitive to Ca^{2+} buffering capacity in the developing rat calyx of Held

R.M. Leão[1,2] and **H. von Gersdorff**[2]

[1]Departamento de Fisiologia, Faculdade de Medicina de Ribeirão Preto, Universidade de São Paulo, Ribeirão Preto, SP, Brasil

[2]The Vollum Institute, Oregon Health and Science University, Portland, OR, USA

Abstract

The calyx of Held, a specialized synaptic terminal in the medial nucleus of the trapezoid body, undergoes a series of changes during postnatal development that prepares this synapse for reliable high frequency firing. These changes reduce short-term synaptic depression during tetanic stimulation and thereby prevent action potential failures during a stimulus train. We measured presynaptic membrane capacitance changes in calyces from young postnatal day 5–7 (p5–7) or older (p10–12) rat pups to examine the effect of calcium buffer capacity on vesicle pool size and the efficiency of exocytosis. Vesicle pool size was sensitive to the choice and concentration of exogenous Ca^{2+} buffer, and this sensitivity was much stronger in younger animals. Pool size and exocytosis efficiency in p5–7 calyces were depressed by 0.2 mM EGTA to a greater extent than with 0.05 mM BAPTA, even though BAPTA is a 100-fold faster Ca^{2+} buffer. However, this was not the case for p10–12 calyces. With 5 mM EGTA, exocytosis efficiency was reduced to a much larger extent in young calyces compared to older calyces. Depression of exocytosis using pairs of 10-ms depolarizations was reduced by 0.2 mM EGTA compared to 0.05 mM BAPTA to a similar extent in both age groups. These results indicate a developmentally regulated heterogeneity in the sensitivity of different vesicle pools to Ca^{2+} buffer capacity. We propose that, during development, a population of vesicles that are tightly coupled to Ca^{2+} channels expands at the expense of vesicles more distant from Ca^{2+} channels.

Keywords

Calyx of Held; Neurotransmission; Calcium buffer; Capacitance measurements; Mammalian auditory brainstem; Synaptic development

Introduction

Action potential invasion of the presynaptic nerve terminal opens voltage-dependent Ca^{2+} channels permitting Ca^{2+} ions to move down their electrochemical gradient into the terminal. Because Ca^{2+} enters via discrete sites, micro-or nanodomains of intracellular Ca^{2+} may form where Ca^{2+} may reach concentrations of 5–10 μM within 200 nm of the channel and up to 100 μM within 20 nm of the channels (1,2). This highly localized peak of synaptic Ca^{2+}

Correspondence to: R.M. Leão, Departamento de Fisiologia, FMRP, USP, Av. Bandeirantes, 3900, 14049-900 Ribeirão Preto, SP, Brasil leaor@fmrp.usp.br.

Presented at the IV Miguel R. Covian Symposium, Ribeirão Preto, SP, Brazil, May 23–25, 2008.

concentration elicits mobilization and fusion of nearby synaptic vesicles. The synapse topography (i.e., the spatial relationship of vesicles to Ca^{2+} channels) is crucial for determining the Ca^{2+}-coupling efficiency of exocytosis, and this relationship seems to vary among different synapses (3). In some synapses, like the squid giant synapse and the chick ciliary ganglion, vesicles are assumed to be in close contact with a single Ca^{2+} channel (4–6). However, at several mammalian central synapses, vesicles are thought to be located far (~200 nm) from Ca^{2+} channels and influenced by overlapping domains of clustered Ca^{2+} channels (3,7), because in these synapses release is very sensitive to relatively slow exogenous Ca^{2+} buffers such as ethylene glycol-bis(2-aminoethyl-ether)-N,N,N',N'-tetraacetic acid (EGTA) (8–10), suggesting that Ca^{2+} ions must travel further to reach their binding sites in the release machinery. Ca^{2+} buffer sensitivity varies between different types of synapses and this can be one factor that determines short-term synaptic plasticity (10–14) and the size of the readily releasable pool of vesicles (15).

The calyx of Held, due to its large size, is accessible to direct electrophysiological recording and has been intensively studied as a model of a fast central synapse (16,17). This synapse undergoes developmental changes during the first two postnatal weeks, which prepare it for mediating high frequency transmission after the onset of hearing at p12 in rodents. In more mature calyces (p12–15), synaptic depression is reduced compared to p5–7 (18), which is proposed to be a consequence of a reduced release probability, a larger vesicle pool size, and a reduced propensity for multivesicular release, which would lead to postsynaptic receptor desensitization (19). The evidence for a smaller pool size in immature synapses comes, in part, from presynaptic capacitance recordings obtained under a single Ca^{2+} buffer condition, namely 0.2 mM EGTA, which is thought to be equivalent to the physiological Ca^{2+} buffer concentration in this synapse (20,21). However, endogenous Ca^{2+} handling changes with development of the calyx: immature terminals have a slower Ca^{2+} extrusion system (22) and weaker expression of Ca^{2+} binding proteins (23,24) compared to more mature synapses. Perhaps because of these changes, short trains of stimuli produce higher levels of intra-calyceal calcium in young calyces than in mature calyces (25). Also, glutamate release from young calyces (p8) is more sensitive to 10 mM EGTA than release from terminals of more mature mice (p18), which exhibited higher Ca^{2+} cooperativity, suggesting tighter coupling of Ca^{2+} channels to release sites in mature synapses (26). Since Ca^{2+} buffering can determine short-term synaptic plasticity (10), developmental changes in this parameter could explain some of decrease in release probability and short-term depression in mature calyces. To investigate this hypothesis further, we measured exocytosis directly using membrane capacitance measurements (C_m) in the calyx of Held during two distinct developmental stages and with three distinct Ca^{2+} buffering conditions. Our aim was to determine the effect of these parameters on exocytotic efficiency, releasable pool size and vesicle pool depletion.

Material and Methods

Slice preparation

Brainstem transverse slices (200 μm thick) were obtained from postnatal day 5 (p5) to p12 Sprague-Dawley rats as described previously (19), and kept in artificial cerebral spinal fluid containing 125 NaCl, 2.5 mM KCl, 1 mM $MgCl_2$, 2 mM $CaCl_2$, 25 mM glucose, 25 mM $NaHCO_3$, 1.25 mM NaH_2PO_4, 0.4 mM ascorbic acid, 3 mM myoinositol, 2 mM Na-pyruvate, pH 7.3, when bubbled with a carbogenic mixture (95% O_2, 5% CO_2).

Whole-cell patch-clamp recording and capacitance measurements

Whole-cell patch-clamp recordings were performed at room temperature (21–23°C) in normal artificial cerebral spinal fluid containing 1 μM tetrodotoxin (TTX) and 10 mM tetraethylammonium chloride (TEA-Cl). The internal solution consisted of 90 mM Cs-

methanesulfonate, 20 mM CsCl, 1 mM $MgCl_2$, 5 mM Na_2-phosphocreatine, 40 mM HEPES, 10 mM TEA-Cl, 0.2 or 5 mM EGTA, or 0.05 mM 1,2-bis(2-aminophenoxy)ethane-N,N,N',N'-tetraacetic acid (BAPTA), 2 mM ATP-Mg, 0.2 mM GTP, pH 7.3, with CsOH, 310 mOsm. Lucifer yellow (0.25 mg/mL) was added to the pipette solution to allow *post hoc* confirmation that the recording was from a calyx. The calyx terminal was held at −70 or −80 mV. Patch pipettes were pulled from soft thin-walled glass (WPI, USA) and had an open tip resistance of 3–7.0 MΩ. Series resistance (7–25 MΩ) was electronically compensated by 30–90%. Data acquisition was controlled by "Pulse" software (Heka, Germany) and signals were recorded via an EPC-9 (Heka) double patch-clamp amplifier. Exocytosis was elicited by single square depolarizations to 0 mV lasting 2, 10, 30, or 90 ms, or by a series of 30 action potential like (AP-like) stimuli (a 1-ms ramp to +40 mV followed by a 1-ms ramp back to the holding potential). This AP-like stimulation produces Ca^{2+} currents that are very similar to those obtained with a calyx AP waveform (Figures 3A and 6 of Ref. 27) generating a Ca^{2+} influx of 1–2 pC per stimulus. Exocytosis was assessed by presynaptic membrane capacitance measurements performed as in Ref. 19 by the "sine + DC" method. Briefly, a sinusoidal voltage command (1 kHz and 60–70 mV peak-to-peak amplitude) was applied to the terminal in addition to the holding command few milliseconds before and after the depolarizing command step. The resulting membrane currents were processed with a software lock-in amplifier (HEKA) that decomposed the current into its resistive and capacitive components, resulting in the calculated series (G_s) and membrane (G_m) conductances and membrane capacitance (C_m). The estimate of the number of vesicles (N_v) was calculated using the formula $N_v = \Delta C_m / (Cm_s \times \pi d^2)$ (28), where *d* is the vesicle diameter and Cm_s is the specific membrane capacitance of 10 fF/μm^2. Vesicle diameter was assumed to be 50 nm in both developmental groups (19). Unpaired t-tests were performed to assess statistical significance of the data and means with two-tail P values below 0.05 were considered to be significantly different. Data were analyzed using IGOR Pro (Wavemetrics). Statistics and curve fitting with a hyperbolic function were performed with Prism (GraphPad). Data are reported as means ± SEM.

Alterations in membrane capacitance in response to the Ca^{2+} currents were not followed by respective calculated changes in series resistance (R_s change after 10 ms Ca^{2+} current was −0.001 ± 0.019 MΩ; Figure 1A; see also Ref. 19). A small current (peak of −37 ± 24 pA after a 100 ms I_{Ca}) that decayed over approximately 200 ms was observed after Ca^{2+} currents longer than 10 ms, and increased linearly with the increase in Ca^{2+} influx, in contrast to the capacitance jump that saturated with long depolarizations (Figure 1C). This current might be attributable to activation of the Na^+/Ca^{2+} exchanger (29) or some other Ca^{2+}-dependent conductance, since it was not observed when the internal solution contained 5 mM EGTA (data not shown). To avoid interference from this conductance in the calculation of membrane capacitance, we collected data after this current had decayed (gray rectangle in Figure 1A).

Time-resolved capacitance measurements using sinusoidal voltage stimuli are based on the assumption that the recorded cell is electrically equivalent to a single compartment composed of a membrane resistor in parallel with a membrane capacitor. Applying a step voltage, via an electrode at the whole-cell voltage-clamp mode, and observing if the resulting capacitive current decays with a single exponential time constant can identify a single-compartment cell (30). Since most calyces included in this study had different axon lengths, based on the lucifer yellow signal and based on the number of exponentials needed to fit the time course of membrane charging currents, most calyces comprised more than one electrical compartment. However, comparison of results from calyces that presented a single electrical compartment to those with more than one electrical compartment showed that Ca^{2+}-dependent capacitance jumps were similar in both groups (data not shown), in agreement with previous observations (19,30).

Results

Calyces of Held nerve terminals were voltage clamped at a holding potential of −80 mV and subjected to step depolarizations to 0 mV of 2- to 90-ms duration. Ca^{2+} currents and corresponding membrane capacitance changes were then recorded (Figure 1B). The resulting capacitance jumps increased with the duration of depolarization, with half-maximal responses occurring at 11 ± 0.3 ms (Figure 1C) and reaching an apparent plateau after 90 ms (Figure 1C). Application of $CdCl_2$ (0.1 mM) abolished both Ca^{2+} currents and capacitance jumps (Figure 1C), as expected if changes in membrane capacitance reflect exocytosis of synaptic vesicles. Recording from postsynaptic cells produced very small capacitance changes (<50 fF after 90-ms depolarizations; Figure 1C), and were thus easily distinguishable from those recorded from calyces. We did not investigate the nature of the postsynaptic capacitance changes further.

Effects of exogenous Ca^{2+} buffer and development on exocytosis

The results illustrated in Figure 1 were recorded using a pipette solution containing 0.2 mM EGTA. Paired recordings indicate that 0.2 mM EGTA and 0.05 mM BAPTA are the approximate endogenous Ca^{2+} buffering in p8–10 calyces for single action potential stimulation (20,21). However, these buffers have quite distinct buffering kinetics, as seen in Figure 6. Due to its faster binding kinetics, 0.05 mM BAPTA is considerably more efficient in buffering Ca^{2+} than four times more EGTA, while 5 mM EGTA is very effective in inhibiting neurotransmission in the calyx of Held (20), although it produces a similar buffering profile as 0.05 mM BAPTA.

These discrepancies might be explained by differences in Ca^{2+} buffer capacity and kinetics. Probably the lower concentration of BAPTA (lower buffering capacity) makes it inefficient in buffering the large local increase in calyceal Ca^{2+} after an action potential, because of quick buffer saturation due to the fast binding rate of Ca^{2+} to BAPTA (10). On the other hand, the larger buffer capacity of 5 mM EGTA and its lower binding kinetics to Ca^{2+} make buffer saturation negligible after Ca^{2+} influx evoked by an action potential. In order to better elucidate the influence of Ca^{2+} buffering capacity on exocytosis in the calyx of Held, and how this relationship is affected during maturation of this synapse, we compared exocytosis in calyces at different stages of maturation (from p5–7 and p10–12 rats) under three Ca^{2+} buffer conditions: 0.05 mM BAPTA, 0.2 mM EGTA and 5 mM EGTA. These age groups were chosen because they flank a period during which the calyx undergoes a rearrangement of exocytotic active zones (19), changes in the coupling of Ca^{2+} entry to exocytosis (25), and changes in the levels of expression of endogenous Ca^{2+} buffers such as parvalbumin (24). All of these factors could lead to changes in the sensitivity of exocytosis to exogenous buffer.

Exocytosis recorded from the two age groups and three buffer conditions are shown in Figure 2A, where the data are plotted versus Ca^{2+} charge (QCa, integral of the Ca^{2+} current) to separate changes in Ca2+ entry from exocytosis efficiency, since Ca^{2+} current amplitude increased during development (data not shown; see Ref. 31). We observed that the maximum number of vesicles released by a long depolarization, as well as the number of vesicles released in response to very short pulses, varied significantly during development.

First it was clear that the maximal capacitance jump (in response to a 90-ms depolarization) was strongly dependent on the choice of Ca^{2+} buffer in p5–7 calyces, with values in 0.05 mM BAPTA approximately two times those obtained with 0.2 mM EGTA (Figure 2; Table 1). In contrast, in p10–12 calyces, maximum capacitance jumps did not differ between the two Ca^{2+} buffer conditions (Figure 2). By converting these capacitance jumps to the number of vesicles (see Methods) we calculate apparent vesicle pool sizes, as shown in Figure 2B and Table 1, showing that the calyces can maximally release about 8500 vesicles when stimulated with our protocol and that this value is reduced by 50% in immature calyces perfused with 0.2

mM EGTA. Increasing the Ca^{2+} buffer to 5 mM EGTA reduced the releasable pool in both age groups to similar levels (down to about 2000 vesicles; Figure 2B and Table 1).

The large difference in vesicle pool generated by 90-ms step depolarizations in 0.05 mM BAPTA versus 0.2 mM EGTA in immature calyces was surprising since these two buffer conditions mimic endogenous buffering for a single action potential stimulation in p8–10 rats (21). We hypothesized that prolonged step depolarizations might evoke exocytosis that is somehow different from what occurs during brief bursts of Ca^{2+} entry during an action potential train. To address this, we first tested whether a train of 30 AP-like stimuli (Figure 3A; see Methods) and a 30-ms step depolarization would evoke exocytosis from a common pool of vesicles. Both protocols elicited similar capacitance jumps (Figure 3B,C; $P > 0.05$). Similar to the response to a step depolarization, exocytosis in response to a train of AP-like stimuli was larger with 0.05 BAPTA as the buffer than with 0.2 mM EGTA in immature calyces (Figure 3C). In all ages and buffer conditions tested, exocytosis evoked by an AP-train was closely correlated with exocytosis evoked by a 30-ms depolarization in the same cell ($r^2 = 0.90$; Figure 3B,D). In addition, exocytosis evoked by a step depolarization was strongly reduced (by 62% on average; N = 3 in 0.05 mM BAPTA and N = 3 in 0.2 mM EGTA; p6-7 calyces) by a preceding train of AP-like stimuli (data not shown). Thus, trains of AP-like stimuli and step depolarizations evoke exocytosis from a common pool of vesicles.

We also observed that, for a given buffer condition, the Ca^{2+} entry required for half-maximum exocytosis (the K_d value obtained from curve fitting) was similar for the different ages studied but was about 50% lower in the low-buffer condition of 0.05 mM BAPTA (15.1 ± 7 pC for p5–7 and 13.95 ± 9 pC for p10–12) compared with 0.2 mM EGTA (24.9 ± 4 pC for p5–7 and 34.3 ± 8 pC for p10–12). This higher potency observed in the low-buffer condition can be better appreciated if we compare the differences in exocytosis during the briefest (2 ms) depolarizations that released a small fraction of the vesicle pool that probably include the vesicles released by a single action potential since this protocol resulted in about 1.5–13.5 pC of Ca^{2+} entry (depending on the age group), or approximately twice the Ca^{2+} entry generated by a single AP (21). A 2-ms depolarization released more vesicles from mature than immature calyces, and in both age groups the calyces released more vesicles in the presence of 0.05 mM BAPTA than in the presence of 0.2 or 5 mM EGTA (Figure 4B;Table 1). Figure 4A shows that in immature calyces 5 mM EGTA was very effective in inhibiting exocytosis by a 2-ms Ca^{2+} current in a p5 calyx in contrast to a p11 calyx. Interestingly, in both age groups, the number of vesicles released by a 2-ms Ca^{2+} current in the presence of 0.05 mM BAPTA was similar to the number of docked vesicles as assayed by electron microscopy (19) (see Figure 4B), suggesting an anatomical correlate for these vesicles.

However, the developmental differences in C_m jumps are perhaps mostly due to the larger Ca^{2+} currents in more mature terminals since when these values were normalized by Q_{Ca} both age groups released a similar number of vesicles under the different buffering conditions, although the release was significantly bigger in the low buffer condition with 0.05 mM BAPTA (Figure 4B, Table 1) than with higher EGTA. It is interesting to note that for a 2-ms depolarization, release per Ca^{2+} ion with 5 mM EGTA (Figure 4B) was not significantly different from that obtained with 0.2 mM EGTA in both age groups, suggesting that 0.2 mM EGTA is sufficient to block the release of all EGTA-sensitive vesicles released during a brief period of Ca^{2+} entry, which is different from what we observed with longer (>10 ms) Ca^{2+} currents.

Effects of exogenous Ca^{2+} buffer on paired-pulse depression

The calyx of Held presents significant synaptic depression in response to high frequency stimulation. We have shown that manipulation of the Ca^{2+} buffer changes the number of vesicles released in response to long and short pulses, and estimates of the apparent pool size

differ depending on the age of the calyx. We next investigated if changes in Ca^{2+} buffer could explain the observed decrease in presynaptic depression that occurs during development. To address this question, we measured capacitance jump depression using two 10-ms depolarizations separated by a 70-ms interval at the holding potential and compared the capacitance jump after each pulse (Figure 5A).

The capacitance change elicited by the second Ca^{2+} current was significantly smaller than the capacitance change produced by the first Ca^{2+} current ($P < 0.0001$; Figure 5B), showing that depression of exocytosis occurs. Increasing Ca^{2+} buffering from 0.05 mM BAPTA to 0.2 mM EGTA significantly decreased capacitance jump depression, independently of the age group (Figure 5C). In 0.05 mM BAPTA, the depression was of 66 ± 7% at p5–7 and 73 ± 7% at p10–12 whereas in 0.2 mM EGTA the depression was of 43 ± 8% at p5–7 and 36 ± 6% at p10–12, values significantly different than those obtained with 0.05 mM BAPTA ($P < 0.05$).

It has been reported that calyceal Ca^{2+} current depression is responsible for short-term depression of neurotransmission in the calyx of Held (32,33). Depression of the presynaptic Ca^{2+} current did occur during most double-pulse protocols (Figure 5B,C), but Ca^{2+} current depression was not significantly different between 0.05 mM BAPTA and 0.2 mM EGTA (depression of I_{Ca}-pre in 0.2 mM EGTA: 11.45 ± 3.7%, in 0.05 mM BAPTA: 15.1 ± 8.1%; $P > 0.05$; Figure 5B), which could not explain the differences observed in paired-pulse depression in these two conditions. Moreover, no correlation was observed between Ca^{2+} current depression and capacitance jump depression ($P = 0.97$; $r^2 = 0.00015$), indicating that Ca^{2+} current depression is not the main factor in producing paired-pulse depression, at least under the present conditions.

Interestingly, we observed that a 10-ms Ca^{2+} current releases about 40% of the total vesicle pool, as calculated by the ratio between the exocytosis induced by a 10- and a 90-ms Ca^{2+} current (Figure 5B). In this situation we would expect a paired-pulse depression of 40%. This agrees with what we observed with 0.2 mM EGTA (Figure 5C) but not with 0.05 mM BAPTA, which produces a more pronounced depression (Figure 5B). We conclude that some other factor in addition to fractional release of the synaptic vesicle pool during the first stimuli and Ca^{2+} current depression determines the extent of paired-pulse depression, and this factor is sensitive to buffers present in the calyx.

Discussion

A developmental increase in the size of the releasable pool and a decrease in the release probability are proposed as adaptive mechanisms to avoid depletion of synaptic vesicle pools in the calyx of Held during high frequency trains of APs (18,19). Here we studied these parameters using direct measurements of vesicle exocytosis, and examined how these parameters were affected by Ca^{2+} buffering capacity in different developmental stages. Recording exocytosis in two different developmental phases of the calyx of Held using three different Ca^{2+} buffering conditions revealed that parameters, such as vesicle pool size, release probability and synaptic depression, are strongly dependent on the Ca^{2+} buffer capacity, especially in immature calyces.

EGTA is a relatively slow buffer and is probably inefficient in buffering the fast rise in Ca^{2+} close to the Ca^{2+} channels after an action potential, although it does inhibit the excitatory postsynaptic current when loaded in the calyx of Held synapses at millimolar concentrations (20,21), suggesting that Ca^{2+} ions must travel some distance in the synapse before reaching the fusion sensor. This result contrasts with observations in the squid giant synapse (4,5) and suggests that the immature calyx of Held does not have an organized distribution of Ca^{2+} channels and vesicles, as reported for other terminals (34,35). Meinrenken et al. (7) developed

a model in which the vesicles in the calyx of Held are randomly located across a cluster of Ca^{2+} channels (with the vesicle distance ranging from 30 to 300 nm) producing overlapping domains of multiple channels controlling vesicle exocytosis, and recruitment of vesicles to these domains has been demonstrated to be a limiting step for exocytosis in the calyx of Held (36). Changes in Ca^{2+} buffering in the terminal could thus strongly modulate vesicle exocytosis. Previous work suggests that immature synapses have a weaker Ca^{2+} buffering system (23,25,31) and less tightly coupled docked vesicles to Ca^{2+} channels (26). Our hypothesis was that these developmental changes in intracellular Ca^{2+} buffering capacity and vesicle coupling could be responsible at least in part for the developmental differences in release probability, vesicle pool size and synaptic depression observed in the calyx of Held synapse.

We used three different mobile Ca^{2+} buffer paradigms. The Ca^{2+} buffering capacity of the three conditions is depicted in Figure 6 where we can see the expected exponential decay of the steady-state Ca^{2+} concentration around the pore of a Ca^{2+} channel in the presence of the three Ca^{2+} buffering conditions. Because BAPTA at the concentration of 0.05 mM is equally effective in buffering Ca^{2+} as EGTA at the concentration of 5 mM, and we observed a facilitating effect of this BAPTA concentration on exocytosis after brief Ca^{2+} currents, we conclude that the fast rise in intracellular Ca^{2+} after a short Ca^{2+} current (e.g., 2 ms) is still able to saturate the smaller concentration of buffer molecules, thus leaving no free buffer molecules for chelating the excess Ca^{2+} influx.

The overall sensitivity of exocytosis to Ca^{2+} buffer capacity (type and concentration of buffer) suggests that the vesicles in the young calyx of Held are loosely coupled to Ca^{2+} channels. Remarkably, in immature terminals low capacity Ca^{2+} buffering reveals a pool of vesicles that are not released in the presence of medium or high buffer capacity, revealing the existence of a group of weakly Ca^{2+}-channel-coupled vesicles that are quite sensitive to slow Ca^{2+} buffers. This pool represents a large fraction of the fast releasable vesicles in immature terminals. Comparing the release per Ca^{2+} ion influx (units of fF/pC) at 2 ms we estimate that the pool of weakly Ca^{2+} channel-coupled vesicles represents 72% of the fast releasing vesicles in the immature synapses, in contrast to 40% of these vesicles in the mature synapses.

It is important to note that the weak Ca^{2+} buffering capacity via 0.05 mM BAPTA could also facilitate exocytosis by different mechanisms such as Ca^{2+}-dependent facilitation and/or potentiation (11,13) by keeping resting or residual Ca^{2+} levels high. This could aid recruitment of vesicles from the reserve to the releasable pool in immature synapses (37) or increase the priming of docked vesicles by increasing Ca^{2+}-dependent DOC2 protein translocation to the membrane (38). Despite these possibilities, we believe that the simplest explanation for the increased exocytosis in immature calyces with 0.05 mM BAPTA is the weaker coupling of vesicles to Ca^{2+} channels.

Another important observation was that the maximal number of vesicles released, or the releasable vesicle pool size, is not a fixed value, but depends on the capacity of the Ca^{2+} buffer system. Also, in immature calyces the size of the releasable pool was more sensitive to increases in Ca^{2+} buffering capacity, suggesting that the releasable vesicle pool undergoes a maturation from very weakly coupled vesicles to more tightly coupled vesicles as the calyx develops, allowing these vesicles to be released even in a stronger Ca^{2+} buffering condition. Taschenberger et al. (19) suggested that a decreased releasable pool in immature terminals was one of the causes of the increased synaptic depression observed in these terminals. On the other hand, our data suggest that the size of the vesicle pool in immature terminals might not be smaller than the one in mature terminals, so that the stronger synaptic depression observed in immature calyces might be generated mainly by an increased release probability due to weaker buffering and/or a larger action potential half-width (18,23,25,31).

The observation that 0.2 mM EGTA is able to inhibit the recruitment of vesicles released after long Ca^{2+} influx (>10 ms) in immature terminals was surprising in light of the fact that during a 50-ms depolarization the resulting Ca^{2+} concentration in the synapse could reach values of approximately 490 μM (assuming a calyx volume of about 0.4 pL) (see Ref. 39), which would be enough to saturate the local 200 μM EGTA (K_d ~176 nM) loaded in the calyx, making this buffer concentration inefficient under such conditions. However, Ca^{2+} extrusion systems such as the Na^+-Ca^{2+} exchanger and Ca^{2+}-pumps (29) could be acting more efficiently during development to speed up Ca^{2+} extrusion from the terminal, so that local Ca^{2+} concentrations never reach such large values.

Finally, we observed an age-independent increase in depression of exocytosis in the presence of a low capacity Ca^{2+} buffer that could not be explained only by increased fractional release of the vesicular pool or increased Ca^{2+} current inactivation. This effect could suggest a form of Ca^{2+}-induced depression or “adaptation” of exocytosis at the calyx of Held synapse. However, it might also reflect the release and depletion of a pool of “reluctant” vesicles with low release probability recruited after the exocytosis of the readily releasable pool of vesicles as observed by Wu and Borst (40). In summary, we note that depression of exocytosis in the calyx of Held is largely dependent on the Ca^{2+} buffering capacity of the terminal.

We conclude that the vesicle pool size of immature calyces is very sensitive to Ca^{2+} buffers and that release probability and synaptic depression are both increased by weak Ca^{2+} buffering capacity at both developmental stages. These effects agree with a model in which exocytosis of synaptic vesicles become more efficient as the synapses mature (19,26). This increased efficiency can be attained by closer proximity of vesicles to Ca^{2+} channels or/and by a developmental change in the intrinsic release probability. Interestingly, in calyces from p8–10 rats, the application of the slow endogenous mobile Ca^{2+} buffer parvalbumin (100 μM) slows down the Ca^{2+} transients after an action potential and reduces paired pulse facilitation in a way similar to that obtained with 0.1 mM EGTA (14). Also, expression of parvalbumin in the auditory system increases during development (23,24), suggesting that a presynaptic increase in parvalbumin expression in the calyx of Held could be a potential mechanism for regulating Ca^{2+} dynamics in this structure.

Acknowledgments

We thank Dr. Christopher Kushmerick (ICB, UFMG, Belo Horizonte, MG, Brazil) for revising and discussing the manuscript.

Research supported by NIH/NIDCD and Pew Foundation grants to H. von Gersdorff. Publication supported by FAPESP.

References

1. Yamada WM, Zucker RS. Time course of transmitter release calculated from simulations of a calcium diffusion model. Biophys J 1992;61:671–682. [PubMed: 1354503]
2. Neher E. Vesicle pools and Ca^{2+} microdomains: new tools for understanding their roles in neurotransmitter release. Neuron 1998;20:389–399. [PubMed: 9539117]
3. Schneggenburger R, Neher E. Presynaptic calcium and control of vesicle fusion. Curr Opin Neurobiol 2005;15:266–274. [PubMed: 15919191]
4. Adams DJ, Takeda K, Umbach JA. Inhibitors of calcium buffering depress evoked transmitter release at the squid giant synapse. J Physiol 1985;369:145–159. [PubMed: 2419546]
5. Adler EM, Augustine GJ, Duffy SN, Charlton MP. Alien intracellular calcium chelators attenuate neurotransmitter release at the squid giant synapse. J Neurosci 1991;11:1496–1507. [PubMed: 1675264]

6. Gentile L, Stanley EF. A unified model of presynaptic release site gating by calcium channel domains. Eur J Neurosci 2005;21:278–282. [PubMed: 15654866]
7. Meinrenken CJ, Borst JG, Sakmann B. Calcium secretion coupling at calyx of Held governed by nonuniform channel-vesicle topography. J Neurosci 2002;22:1648–1667. [PubMed: 11880495]
8. Atluri PP, Regehr WG. Delayed release of neurotransmitter from cerebellar granule cells. J Neurosci 1998;18:8214–8227. [PubMed: 9763467]
9. Chen C, Regehr WG. Contributions of residual calcium to fast synaptic transmission. J Neurosci 1999;19:6257–6266. [PubMed: 10414955]
10. Rozov A, Burnashev N, Sakmann B, Neher E. Transmitter release modulation by intracellular Ca^{2+} buffers in facilitating and depressing nerve terminals of pyramidal cells in layer 2/3 of the rat neocortex indicates a target cell-specific difference in presynaptic calcium dynamics. J Physiol 2001;531:807–826. [PubMed: 11251060]
11. Sakaba T, Neher E. Quantitative relationship between transmitter release and calcium current at the calyx of Held synapse. J Neurosci 2001;21:462–476. [PubMed: 11160426]
12. Awatramani GB, Price GD, Trussell LO. Modulation of transmitter release by presynaptic resting potential and background calcium levels. Neuron 2005;48:109–121. [PubMed: 16202712]
13. Korogod N, Lou X, Schneggenburger R. Presynaptic Ca^{2+} requirements and developmental regulation of posttetanic potentiation at the calyx of Held. J Neurosci 2005;25:5127–5137. [PubMed: 15917453]
14. Muller M, Felmy F, Schwaller B, Schneggenburger R. Parvalbumin is a mobile presynaptic Ca^{2+} buffer in the calyx of Held that accelerates the decay of Ca^{2+} and short-term facilitation. J Neurosci 2007;27:2261–2271. [PubMed: 17329423]
15. Burrone J, Neves G, Gomis A, Cooke A, Lagnado L. Endogenous calcium buffers regulate fast exocytosis in the synaptic terminal of retinal bipolar cells. Neuron 2002;33:101–112. [PubMed: 11779483]
16. Forsythe ID. Direct patch recording from identified presynaptic terminals mediating glutamatergic EPSCs in the rat CNS, in vitro. J Physiol 1994;479(Part 3):381–387. [PubMed: 7837096]
17. Schneggenburger R, Forsythe ID. The calyx of Held. Cell Tissue Res 2006;326:311–337. [PubMed: 16896951]
18. Taschenberger H, von Gersdorff H. Fine-tuning an auditory synapse for speed and fidelity: developmental changes in presynaptic waveform, EPSC kinetics, and synaptic plasticity. J Neurosci 2000;20:9162–9173. [PubMed: 11124994]
19. Taschenberger H, Leao RM, Rowland KC, Spirou GA, von Gersdorff H. Optimizing synaptic architecture and efficiency for high-frequency transmission. Neuron 2002;36:1127–1143. [PubMed: 12495627]
20. Borst JG, Sakmann B. Calcium influx and transmitter release in a fast CNS synapse. Nature 1996;383:431–434. [PubMed: 8837774]
21. Borst JG, Helmchen F, Sakmann B. Pre- and postsynaptic whole-cell recordings in the medial nucleus of the trapezoid body of the rat. J Physiol 1995;489(Part 3):825–840. [PubMed: 8788946]
22. Chuhma N, Koyano K, Ohmori H. Synchronisation of neurotransmitter release during postnatal development in a calyceal presynaptic terminal of rat. J Physiol 2001;530:93–104. [PubMed: 11136861]
23. Lohmann C, Friauf E. Distribution of the calcium-binding proteins parvalbumin and calretinin in the auditory brainstem of adult and developing rats. J Comp Neurol 1996;367:90–109. [PubMed: 8867285]
24. Felmy F, Schneggenburger R. Developmental expression of the Ca^{2+}-binding proteins calretinin and parvalbumin at the calyx of Held of rats and mice. Eur J Neurosci 2004;20:1473–1482. [PubMed: 15355314]
25. Nakamura T, Yamashita T, Saitoh N, Takahashi T. Developmental changes in calcium/calmodulin-dependent inactivation of calcium currents at the rat calyx of Held. J Physiol 2008;586:2253–2261. [PubMed: 18238813]
26. Fedchyshyn MJ, Wang LY. Developmental transformation of the release modality at the calyx of Held synapse. J Neurosci 2005;25:4131–4140. [PubMed: 15843616]

27. Leao RM, von Gersdorff H. Noradrenaline increases high-frequency firing at the calyx of Held synapse during development by inhibiting glutamate release. J Neurophysiol 2002;87:2297–2306. [PubMed: 11976369]
28. Sun JY, Wu LG. Fast kinetics of exocytosis revealed by simultaneous measurements of presynaptic capacitance and postsynaptic currents at a central synapse. Neuron 2001;30:171–182. [PubMed: 11343653]
29. Wolfel M, Schneggenburger R. Presynaptic capacitance measurements and Ca^{2+} uncaging reveal submillisecond exocytosis kinetics and characterize the Ca^{2+} sensitivity of vesicle pool depletion at a fast CNS synapse. J Neurosci 2003;23:7059–7068. [PubMed: 12904466]
30. Sun JY, Wu XS, Wu W, Jin SX, Dondzillo A, Wu LG. Capacitance measurements at the calyx of Held in the medial nucleus of the trapezoid body. J Neurosci Methods 2004;134:121–131. [PubMed: 15003378]
31. Chuhma N, Ohmori H. Postnatal development of phase-locked high-fidelity synaptic transmission in the medial nucleus of the trapezoid body of the rat. J Neurosci 1998;18:512–520. [PubMed: 9412527]
32. Forsythe ID, Tsujimoto T, Barnes-Davies M, Cuttle MF, Takahashi T. Inactivation of presynaptic calcium current contributes to synaptic depression at a fast central synapse. Neuron 1998;20:797–807. [PubMed: 9581770]
33. Xu J, Wu LG. The decrease in the presynaptic calcium current is a major cause of short-term depression at a calyx-type synapse. Neuron 2005;46:633–645. [PubMed: 15944131]
34. Harlow ML, Ress D, Stoschek A, Marshall RM, McMahan UJ. The architecture of active zone material at the frog's neuromuscular junction. Nature 2001;409:479–484. [PubMed: 11206537]
35. Dresbach T, Qualmann B, Kessels MM, Garner CC, Gundelfinger ED. The presynaptic cytomatrix of brain synapses. Cell Mol Life Sci 2001;58:94–116. [PubMed: 11229820]
36. Wadel K, Neher E, Sakaba T. The coupling between synaptic vesicles and Ca^{2+} channels determines fast neurotransmitter release. Neuron 2007;53:563–575. [PubMed: 17296557]
37. Becherer U, Moser T, Stuhmer W, Oheim M. Calcium regulates exocytosis at the level of single vesicles. Nat Neurosci 2003;6:846–853. [PubMed: 12845327]
38. Friedrich R, Groffen AJ, Connell E, van Weering Jr, Gutman O, Henis YI, et al. DOC2B acts as a calcium switch and enhances vesicle fusion. J Neurosci 2008;28:6794–6806. [PubMed: 18596155]
39. Helmchen F, Borst JG, Sakmann B. Calcium dynamics associated with a single action potential in a CNS presynaptic terminal. Biophys J 1997;72:1458–1471. [PubMed: 9138591]
40. Wu LG, Borst JG. The reduced release probability of releasable vesicles during recovery from short-term synaptic depression. Neuron 1999;23:821–832. [PubMed: 10482247]

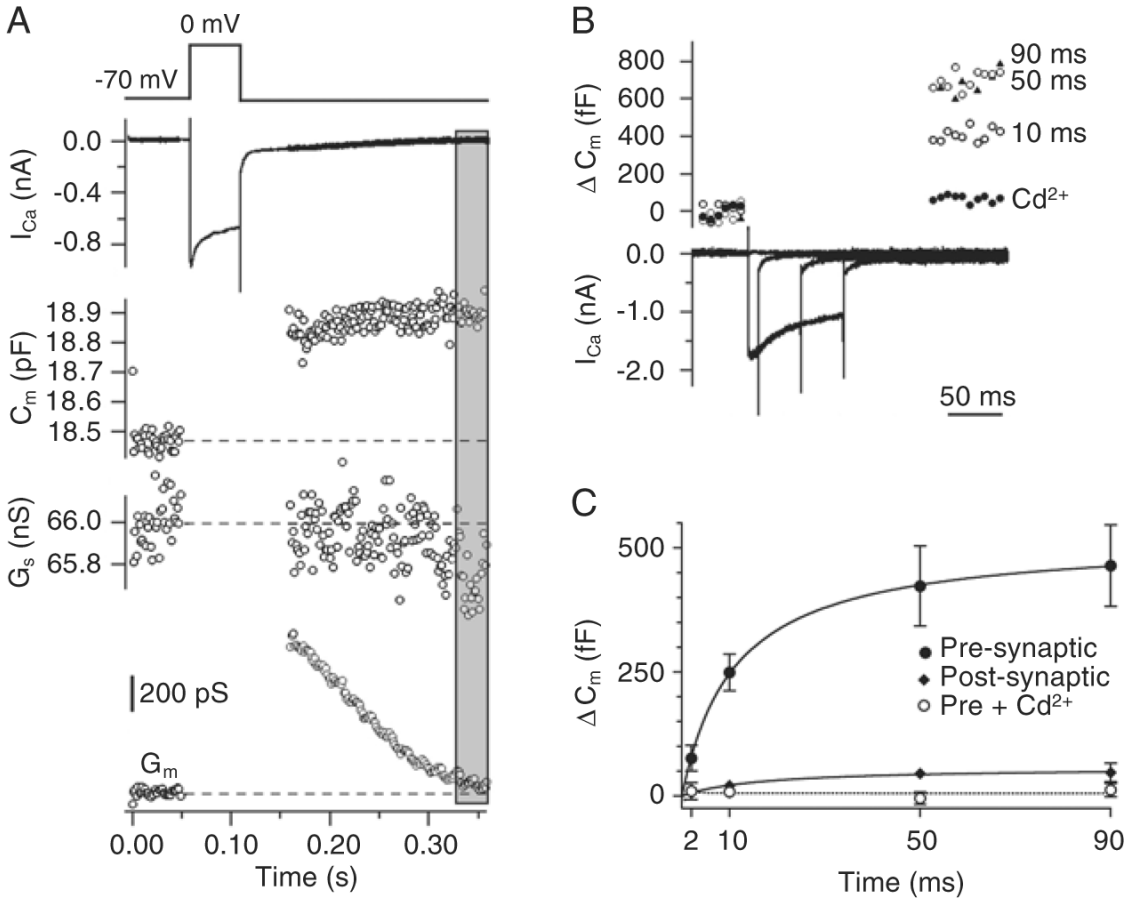

Figure 1.

Measuring exocytosis using membrane capacitance changes in p8–10 rats. The internal Ca^{2+} buffer was 0.2 mM EGTA. *A*, Changes of membrane capacitance (C_m), series conductance (G_s) and membrane conductance (G_m) evoked by a 90-ms Ca^{2+} current (top trace). The area in the gray rectangle shows the time window used to measure membrane capacitance. *B*, Example of the response to presynaptic Ca^{2+} currents evoked by a depolarization to 0 mV of 10-, 50- and 90-ms duration. In the presence of 100 μM $CdCl_2$, no Ca^{2+} current or capacitance jump was detected. *C*, The average capacitance jumps from 10 synapses (means ± SEM). Presynaptic cell (control conditions; filled circles); presynaptic cell in the presence of $CdCl_2$ (0.1 mM; open circles), postsynaptic cell (lozenges). The curves are fit to a square hyperbolic function.

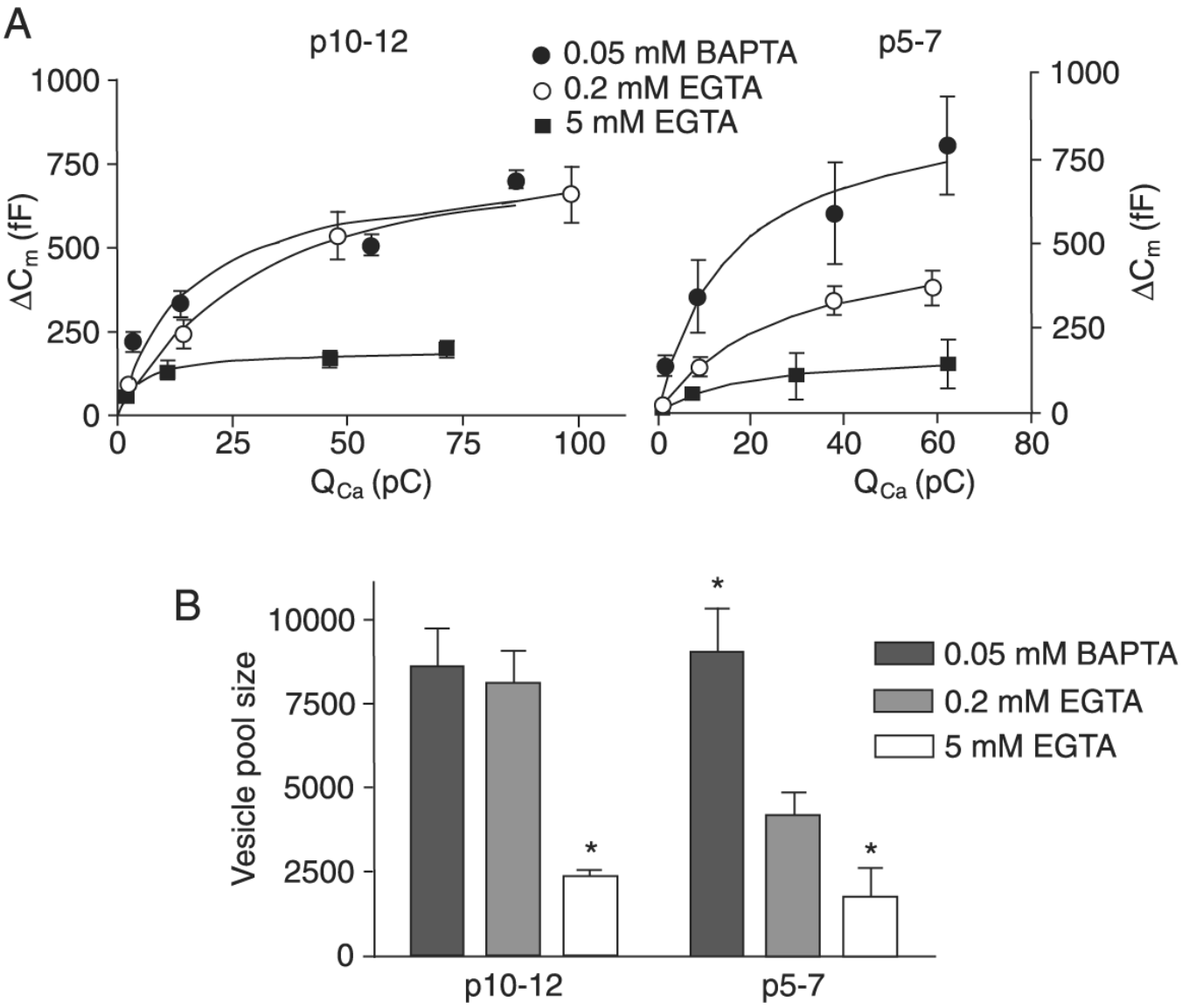

Figure 2.

Membrane capacitance changes (ΔC_m) in immature (p5–7) and more mature terminals (p10–12) under different Ca^{2+} buffering conditions. *A*, Plot of membrane capacitance in response to different Ca^{2+} current charge transfer (integrals of the Ca^{2+} current). The points correspond to I_{Ca} elicited by 2-, 10-, 50-, and 90-ms step pulses to 0 mV. The curves were fitted using a square hyperbolic function. Data are reported as means ± SEM. *B*, Changes in vesicle pool size (ΔC_m elicited by a 90-ms pulse) for two age groups and different Ca^{2+} buffering conditions. *P < 0.05, significantly different compared to other buffer conditions in the same age group (unpaired *t*-test). N = 7–8 calyces for each age group (0.05 mM BAPTA; 0.2 mM EGTA) and N = 3 calyces for each age group for 5 mM EGTA.

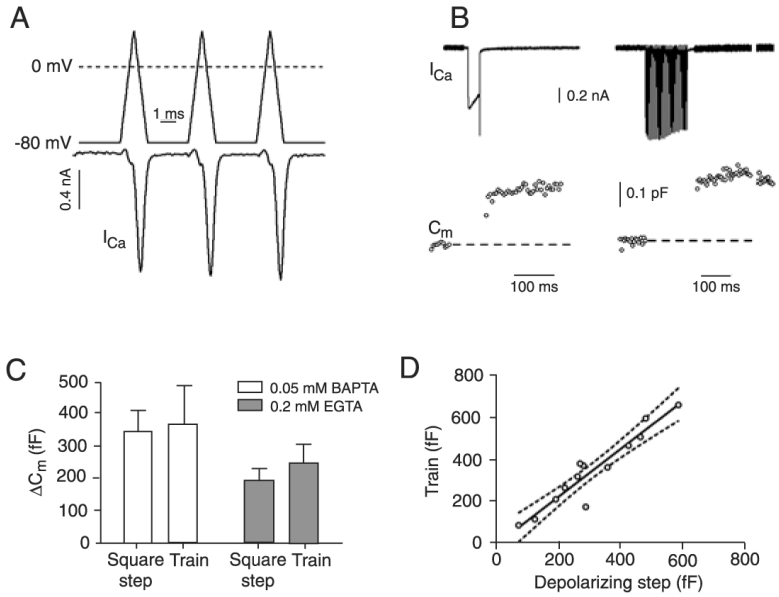

Figure 3.

A, Action potential (AP)-like commands and elicited Ca^{2+} currents. *B*, Ca^{2+} currents (I_{Ca}) and capacitance jumps (C_m) elicited by a 30-ms square depolarization to 0 mV and by a 300 Hz train of 30 AP-like pulses. *C*, Comparison of the capacitance changes (ΔC_m)elicited by the 30-ms Ca^{2+} current (square step) and by the 300 Hz train of AP-like stimuli (train) in 0.05 mM BAPTA and 0.2 mM EGTA. Data are reported as means ± SEM. *D*, Relationship between the capacitance changes elicited by the, 30-ms Ca^{2+} current (depolarizing step) and by the 300 Hz train of AP-like stimuli (train). The line is a linear regression and the dashed lines the 95% confidence intervals.

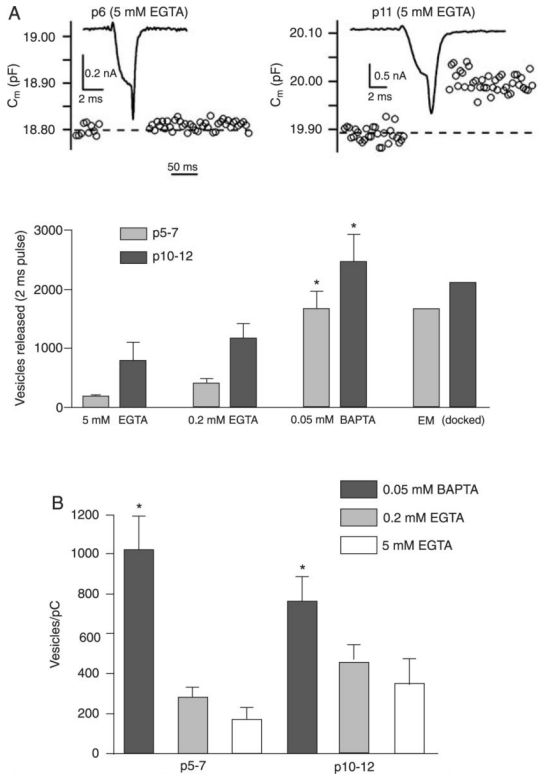

Figure 4.

A, Examples of capacitance jumps (C_m) evoked by a 2-ms Ca^{2+} current in a p6 calyx (left) and a p11 calyx (right) loaded with 5 mM EGTA (note different time scale bars for Ca^{2+} current and capacitance measurements). The average number of vesicles released by a 2-ms depolarization is shown for different buffer conditions. The number of docked vesicles estimated by electron microscopy (EM) is from Taschenberger et al. (19). Data are reported as means ± SEM.*P < 0.05, significantly different from the other buffer conditions (unpaired *t*-test). *B*, Changes in exocytosis per Ca^{2+} ion influx (vesicles/pC of I_{Ca} for 2 ms pulse; *P < 0.05, significantly different from the other buffer conditions; unpaired *t*-test).

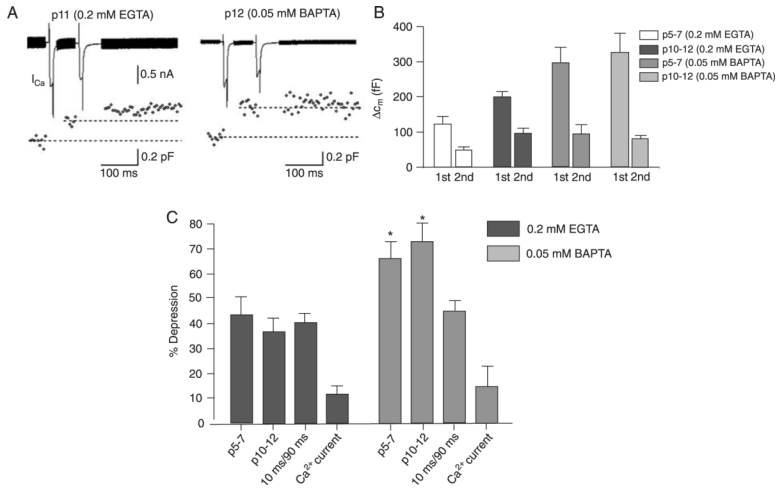

Figure 5.

Changes in paired-pulse depression. *A*, Two 10-ms Ca^{2+} currents (ICa) were delivered 70 ms apart (top trace) and the capacitance changes (bottom trace) were measured. Each capacitance point is the average of five consecutive data points. *B*, Comparison of capacitance changes (ΔC_m) elicited by the first and the second 10-ms Ca^{2+} current in each age group and buffer condition. *C*, Depression of exocytosis and of Ca^{2+} current. Exocytosis from calyces: N = 8 (0.2 mM EGTA p10–12), N = 10 (0.2 mM EGTA p5–7), N = 8 (0.05 mM BAPTA p10–12), N = 5 (0.05 mM BAPTA p5–7); Ca^{2+} current of calyces: N = 5 (0.2 mM EGTA p10–12), N = 5 (0.05 mM BAPTA p10–12). Data are reported as means ± SEM. *P < 0.05 compared with 0.2 mM EGTA (unpaired *t*-test).

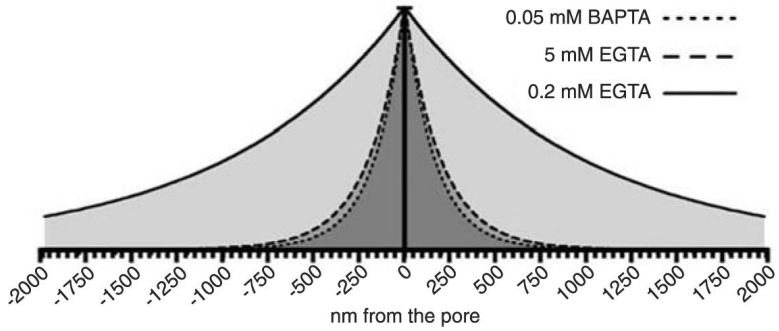

Figure 6.

Calculated radial decay of steady-state Ca^{2+} around the channel pore under the influence of the three Ca^{2+} buffers used: 0.05 mM BAPTA, 0.2 and 5 mM EGTA. The decay was calculated as described in Ref. 2 using a single exponential decay function with a space constant (λ) calculated using the formula: $\lambda = (D_{Ca}\tau)^{1/2}$, where D_{Ca} is the diffusion coefficient of Ca^{2+} and τ is a time constant calculated using the formula: $\tau = 1/(k_{on}B)$, where k_{on} is the buffer association constant and B is the buffer concentration. Values used were: $D_{Ca} = 5{\cdot}10^{-6}{\cdot}cm^{-1}$; $k_{onBAPTA} = 4{\cdot}10^{8}\ M^{-1}{\cdot}s^{-1}$; $k_{onEGTA} = 2.5{\cdot}10^{6}\ M^{-1}{\cdot}s^{-1}$.

Table 1

Vesicles released by step depolarization and number of docked vesicles estimated by electron microscopy.

Step	p5–7 vesicles			p10–12 vesicles		
	EGTA (0.2 mM)	BAPTA (0.05 mM)	EGTA (5 mM)	EGTA (0.2 mM)	BAPTA (0.05 mM)	EGTA (5 mM)
2 ms	406	1684	160	1166	2667	781
10 ms	1696	4160	671	2973	4049	1684
50 ms	4048	7176	1344	6517	6156	2022
90 ms	4491	8943	1773	8052	8560	2358
Docked (EM)		1670			2100	

The number of vesicles was obtained by multiplying the capacitance jump (in fF) by the factor 12.2. The number of docked vesicles was determined by electron microscopy (EM) as described by Taschenberger et al. (19).